Computer Physics Communications 204 (2016) 31–37

Contents lists available at ScienceDirect

Computer Physics Communications

journal homepage: www.elsevier.com/locate/cpc

Stochastic kinetic mean field model

Zoltán Erdélyi [a,*], Mykola Pasichnyy [b], Volodymyr Bezpalchuk [b], János J. Tomán [a], Bence Gajdics [a], Andriy M. Gusak [b]

[a] Department of Solid State Physics, University of Debrecen, P.O. Box 2, H-4010 Debrecen, Hungary

[b] Department of Physics, Cherkasy National University, Shevchenko Street 81, Cherkasy 18031, Ukraine

ARTICLE INFO

Article history:
Received 14 October 2015
Received in revised form
23 February 2016
Accepted 9 March 2016
Available online 6 April 2016

Keywords:
A fluctuation phenomena
Random processes
Noise
Brownian motion
Computational techniques
Simulations
Statistical mechanics of model systems (Ising model, Potts model, field-theory models, Monte Carlo techniques, etc.)
Nucleation

ABSTRACT

This paper introduces a new model for calculating the change in time of three-dimensional atomic configurations. The model is based on the kinetic mean field (KMF) approach, however we have transformed that model into a stochastic approach by introducing dynamic Langevin noise. The result is a stochastic kinetic mean field model (SKMF) which produces results similar to the lattice kinetic Monte Carlo (KMC). SKMF is, however, far more cost-effective and easier to implement the algorithm (open source program code is provided on http://skmf.eu website). We will show that the result of one SKMF run may correspond to the average of several KMC runs. The number of KMC runs is inversely proportional to the amplitude square of the noise in SKMF. This makes SKMF an ideal tool also for statistical purposes.

1. Introduction

Mean field approach to the thermodynamics of phase transformations in solids has been well-known for years [1]. It was developed into Generalized Stochastic Field Kinetic Model by inclusion of the Langevin noise of conserved (composition) and non-conserved order parameters. [2,3]. Noise amplitude satisfied the fluctuation–dissipation theorem and was determined by the temperature and mobility. Among attempts of non-linear generalization to kinetics of diffusion controlled processes—the most well-known now (and self-consistent)—is a quasi-one-dimensional model by George Martin [4]. Martin's kinetic mean field model (KMF) was developed from the very beginning for atomic scale (at the base of master equation) and took into account the dependence of jump frequencies (and corresponding activation energies) on the local surrounding of jumping atoms. Note that in Martin's atomistic model one does not need any additional non-conserved order parameter to describe ordering of alloy—it is fully described by distribution of composition (conserved parameter) at each site. This model did not contain noise and was applied not only to phase transformations but also to initial stages of diffusion. The most interesting results were obtained for systems with a large asymmetry of components (large difference between A–A and B–B pair interaction energies) [5,6]. In particular, asymmetry may lead to sharpening of composition profile instead of its smoothening (of course, simultaneously with its movement due to intermixing). Also, formation of intermediate B2 ordered phase in the contact zone of the couple with sharp asymmetry may start far from stoichiometric composition [7]. In [8] this approach was modified to 3D case.

All systems treated by KMF, may be alternatively treated by KMC [9,10]. The main advantage of algorithms based on the kinetic mean field (KMF) approximation is that they give definite results. We do not need to run the algorithm several times and then average them to predict the most probable scenario of a process. They have, however, a significant drawback: stochastic fluctuations induced processes cannot be simulated. For instance, nucleation of precipitates in a supersaturated solid solution outside of the spinodal will never occur in a mean field model. Moreover, a random solid solution (described in KMF by absolutely the same composition at all sites) quenched into the spinodal region will never decompose. Therefore, if evolution of the system includes overcoming of some barrier via some saddle point with

* Corresponding author.
E-mail address: zoltan.erdelyi@science.unideb.hu (Z. Erdélyi).

http://dx.doi.org/10.1016/j.cpc.2016.03.003
0010-4655/

further normal decrease of free energy, the KMF method fails. Overcoming of the (nucleation) barrier is an important stage of the first order transformation. Introduction of noise into the kinetic mean field model provides the possibility of first order phase transformations but still keeps the advantages of KMF.

2. Methods

The problem of noise is well-known from Brownian motion. It is important to introduce the stochastic factor into a deterministic scheme keeping the phase trajectories continuous—excluding the possibility of jumps in the phase space. Therefore the noise is prescribed neither to coordinates nor to velocities but to forces (or accelerations). Force acting on the Brownian particle is represented as the sum of two forces: viscous and stochastic. Substituting them into Newton's second law:

$$\frac{d\overrightarrow{v}}{dt} = -\gamma\overrightarrow{v} + \frac{\overrightarrow{F}_{stoch}}{m}$$

where γ is a damping coefficient. Stochastic force $\overrightarrow{F}_{stoch}$ and corresponding stochastic acceleration $\overrightarrow{a}_{stoch} = \overrightarrow{F}_{stoch}/m$ are treated as random variables with zero time correlation. Accordingly, the correlation function has the form of Dirac delta-function:

$$\left\langle \overrightarrow{a}_{stoch}(t), \overrightarrow{a}_{stoch}\left(t'\right)\right\rangle = A_n\delta\left(t-t'\right)$$

where $<>$ means averaging over ensemble or – according to ergodic hypothesis – over time, and A_n is the amplitude of the noise. In numeric solution, when the time is discrete with time step dt:

$$\left\langle \overrightarrow{a}_{stoch}(t_i), \overrightarrow{a}_{stoch}\left(t_j\right)\right\rangle = \frac{A_n}{dt}\delta_{i,j}.$$

In such representation the results (average values) will not depend on the time step. Physically it means that we fix the change of velocity during one time step. Such noise without memory is called a Langevin noise. Noise amplitude is determined from the constraint of thermodynamic equilibrium between the ensemble of Brownian particles and the surrounding fluctuating medium.

We will introduce the noise into mean field kinetic equations taking into account that these equations contain only first time derivative instead of second one (no inertia). Accordingly, one might assume that the noise amplitude should be divided not by dt but by $\sqrt{dt}$. One must also decide the noise of WHAT should be introduced. Noise (random change) of composition in each site at each time moment is not the best idea, since it immediately leads to singularities in the composition change rates. Accordingly, noise must be prescribed to the REASON of change in composition—to the microfluxes between neighboring sites. Actually, it is a noise of jump frequencies. This can be introduced in at least two ways: random addition to deterministic frequencies or random change of activation energy in the expression for jump frequency. In this paper we will demonstrate the first way.

Rate of change of composition in each site i of a three-dimensional grid is defined according to conservation of matter and the corresponding local flux balance at each site (in the case of the exchange mechanism of diffusion):

$$\frac{dc_i}{dt} = -\sum_{j=1}^{Z}\left[c_i\left(1-c_j\right)\left(\Gamma_{i,j}^{mean\text{-}field} + \delta\Gamma_{i,j}^{Lang}\right) - \left(1-c_i\right)c_j\left(\Gamma_{j,i}^{mean\text{-}field} + \delta\Gamma_{j,i}^{Lang}\right)\right] \quad (1)$$

where c_i is the atomic fraction of A atoms at site i, c_j is the atomic fraction of A atoms on a neighboring site j, and the total number of nearest neighbors is Z. $c_i\left(1-c_j\right)$ is in fact the probability that the site i is occupied by an A atom and a neighboring j site by a B atom; i.e. an A–B exchange is possible. (In mean field approximation the correlations are neglected.) $\Gamma_{i,j}^{mean\text{-}field}$ is the probability of such an exchange per unit time in mean field approximation, i.e. the jump rate of A atoms from site i to a neighboring site j and backward jumps of B atoms ($\Gamma_{j,i}^{mean\text{-}field}$ is for an exchange of an A and a B atoms being on site j and i, respectively):

$$\Gamma_{i,j}^{mean\text{-}field} = \nu\ \exp\left(\frac{-Q_{i,j}}{kT}\right) = \nu\ \exp\left(-\frac{E_0 - E_{i,j}}{kT}\right).$$

Here k is Boltzmann's constant, T is the absolute temperature, $Q_{i,j} = E_0 - E_{i,j}$, E_0 is the saddle point energy, considered constant in this work, and $E_{i,j} = E_i^A + E_j^B$ where $E_i^A = \sum_{l=1}^{Z}[c_l V_{AA} + (1-c_l)V_{AB}]$ and $E_j^B = \sum_{n=1}^{Z}[c_n V_{AB} + (1-c_n)V_{BB}]$ are the interaction energies of an A and a B atom on site i and j, respectively; $V_{\alpha\beta}$ $(\alpha, \beta = A, B)$ are the pair interaction energies. On introducing $M = (V_{AA} - V_{BB})/2$, $V = V_{AB} - (V_{AA} + V_{BB})/2$ and $\Gamma_0 = \nu \exp\{[-E_0 + Z(V_{AB} + V_{BB})]/kT\}$, $\Gamma_{i,j}^{mean\text{-}field}$ can also be written as:

$$\Gamma_{i,j}^{mean\text{-}field} = \Gamma_0 \exp\left(\frac{\hat{E}_{i,j}}{kT}\right) \quad (2)$$

where

$$\hat{E}_{i,j} = (M-V)\sum_{l=1}^{Z} c_l + (M+V)\sum_{n=1}^{Z} c_n. \quad (3)$$

Note that V is the regular solid solution parameter – proportional to the heat of mixing – and M determines the strength of the composition dependence of the tracer diffusion coefficient (diffusion asymmetry). Last but not least, $\delta\Gamma^{Lang}$ in Eq. (1) are the noise terms, which are random additions to the mean field exchange rates:

$$\delta\Gamma_{i,j}^{Lang} = \frac{A_n}{\sqrt{dt}}\sqrt{3}\,(2random - 1) \quad (4)$$

where random is a uniform random number between 0 and 1. It is easy to check that the random expression $\sqrt{3}\,(2random - 1)$ has the mean squared value equal to 1. Note that thanks to the $\sqrt{dt}$ in denominator of Eq. (4) the asymptotic dispersion of concentration at fixed A_n does not depend on dt.

Actually, Eqs. (1)–(4) have to be used to calculate the time evolution of the composition at each site of a 3D lattice (see open source code). With $A_n = 0$, we perform a fully mean field calculation, whereas with increasing A_n the calculation becomes more and more stochastic, that is the dispersion of composition becomes higher.

Formally, it is possible to rewrite the master equations for the vacancy mechanism:

$$\frac{dc_A(i)}{dt} = -c_A(i)\sum_{j=1}^{Z} c_v(k)\Gamma_{ij}^{AV} + c_v(i)\sum_{j=1}^{Z} c_A(k)\Gamma_{ji}^{AV}$$

$$\frac{dc_B(i)}{dt} = -c_B(i)\sum_{j=1}^{Z} c_v(j)\Gamma_{ij}^{BV} + c_v(i)\sum_{j=1}^{Z} c_B(j)\Gamma_{ji}^{BV},$$

$$\frac{dc_v(i)}{dt} = -c_v(i)\sum_{j=1}^{Z} c_A(j)\Gamma_{ji}^{AV} - c_v(i)\sum_{j=1}^{Z} c_B(j)\Gamma_{ji}^{BV} + c_A(i)\sum_{j=1}^{Z} c_v(j)\Gamma_{ij}^{AV} + c_B(i)\sum_{j=1}^{Z} c_v(j)\Gamma_{ij}^{BV}.$$

Here

$$\Gamma_{ij}^{AV} = \nu_A \exp\left(-\frac{E_0 - E_i^A}{kT}\right),$$

$$\Gamma_{ij}^{BV} = \nu_B \exp\left(-\frac{E_0 - E_i^B}{kT}\right),$$

$$E_i^A = \sum_{l=1}^{Z} [c_A(l)V_{AA} + c_B(l)V_{AB}],$$

$$E_i^B = \sum_{l=1}^{Z} [c_A(l)V_{BA} + c_B(l)V_{BB}].$$

Nevertheless, such a formal approach is almost useless as the time step is determined by the fastest component. In this case vacancies are by many orders of magnitude faster than A and B. Therefore it is practically impossible to calculate the redistribution of the main components in reasonable computation time. To escape this problem, we suggest using the steady-state approximation for vacancies:

$$\frac{dc_v(i)}{dt} = 0.$$

This approximate equation can be used as a basis for iteration procedure:

$$c_v^{iter+1}(i) = \frac{c_A(i)\sum_{j=1}^{Z} c_v^{iter}(j)\Gamma_{ij}^{AV} + c_B(i)\sum_{j=1}^{Z} c_v^{iter}(j)\Gamma_{ij}^{BV}}{\sum_{j=1}^{Z}\left[c_A(j)\Gamma_{ji}^{AV} + c_B(j)\Gamma_{ji}^{BV}\right]}.$$

3. Algorithm

In this paper we show the algorithm for the exchange mechanism. At a later date we will publish the code for the vacancy mechanism.

To calculate the time evolution of the composition at each site, we have to solve Eq. (1). In fact, the first and second terms in Eq. (1) are the outgoing and incoming net fluxes of A atoms, respectively. It is, however, very important to emphasize that the incoming net flux for a site is also an outgoing one for the neighboring sites and vice versa. As a consequence, it is purposeful to construct the algorithm in a way where one calculates only the outgoing fluxes at every site to the neighboring sites. To solve Eq. (1), we use its dimensionless form. Accordingly, we introduced the dimensionless time $\tau \equiv \Gamma_0 t$, noise amplitude $\tilde{A}_n \equiv A_n/\sqrt{\Gamma_0}$ and frequency $\tilde{\Gamma}_{i,j}^{mean\text{-}field} \equiv \Gamma_{i,j}^{mean\text{-}field}/\Gamma_0$.

A basic open source code is available on the http://skmf.eu website. It serves demonstrational purposes to help in understanding how SKMF works; it is not optimized for efficiency but for understanding. The program's input is in ASCII format (input.txt). In the input file the following parameters should be given: seed for the pseudorandom number generator (0 gives pseudorandom seed), dimensions of the FCC crystal lattice sample (Nx, Ny, Nz), where the unit cell's dimensions are $2 \times 2 \times 2$. Note that because of the periodic boundary conditions applied in the software, input dimensions should be even numbers in all three directions. This way the number of particles in such a system is given by $N_x \times N_y \times N_z/2$. The next two parameters are the dimensionless diffusion asymmetry parameter (M/kT) and dimensionless regular solid solution parameter (V/kT). The dimensionless amplitude of dynamic Langevin noise (An_tilde) and the value of the dimensionless time step (dtau) should be given in the next two lines. The recording frequency (Ss) and the total number of records (Ns not including the initial state) provide the possibility to adjust the length of the simulation and the time resolution. The consecutive composition configurations are recorded into an output file (output.xyz) formatted for direct use in Ovito (Open Visualization Tool [11]). The last input parameter determines the average composition of the system, which is the starting atomic fraction at every site in the case of a homogeneous initial state.

It is important to note that if the composition fluctuations caused by the amplitude of Langevin noise are high enough compared to the values of c_i or $1 - c_i$, the fluctuations can lead the composition of site i out of the [0,1] range – as the noise is independent of the local composition. This situation, being unphysical, requires some action. Two main approaches are possible to handle this phenomenon. First, to prevent such a situation by changing the Langevin noise depending on how close the composition of a site and its surrounding are to 0 or 1. Second, to leave the noise unaffected, but after updating the concentrations, the material outside [0,1] interval should somehow be redistributed in the system in a physically meaningful way. From a computational point of view, the second approach is simpler and more straightforward. We implemented the latter one.

The main idea is to divide one computational cycle into two parts: mean field and noise. In one iteration cycle, we first calculate dc_i from Eq. (1) supposing that $\delta\Gamma_{i,j}^{Lang} = 0$ for all i, j (denote this by $dc_i^{mean\text{-}field}$) and check if all c_i would remain in the range of [0,1] after updating the composition; but we do not update the composition at this point. If the composition is not in range, then KMF solution is not stable, the software needs to be restarted with decreased time step. If, however, the composition remains in the [0,1] range everywhere, we calculate dc_i from Eq. (1) again but now supposing that $\Gamma_{i,j}^{mean\text{-}field} = 0$ for all i, j (denote this by dc_i^{Lang}). We now update c_i by $dc_i = dc_i^{mean\text{-}field} + dc_i^{Lang}$ and check if the updated values are in the range of [0,1]. If it is not in range, we redistribute the excess ($c_i > 1$; or deficiency $c_i < 0$) material among the neighboring sites. The redistribution is not even but weighted by the composition of the sites. For safety's sake, after redistribution we check again if the composition of all sites is in the [0,1] range; if not, the software needs to be restarted with a decreased time step.

It is very important to note that it is only necessary to apply this redistribution algorithm if the studied problem leads to compositions close to 0 or 1. For example, in this work we needed to apply this only for the case of calculation of phase separation from supersaturated homogeneous alloy with very limited solubility (see later).

In stochastic models good quality pseudorandom numbers are needed. In the published code we used the Mersenne-Twister MT19937 [12] algorithm via the standard C++11 implementation.

4. Results and discussion

As shown in Appendix A, the interrelation between noise amplitude and composition fluctuations can be derived analytically for the simplest case of ideal ($V = 0$) and symmetric ($M = 0$) solution (in this case the base exchange frequency – without noise – is equal to Γ_0 for all possible exchanges, and its dimensionless counterpart $\tilde{\Gamma} \equiv \tilde{\Gamma}_{i,j}^{mean\text{-}field} = \Gamma_0/\Gamma_0 = 1$ for all i, j):

$$\sqrt{\langle(\delta c)^2\rangle} = \frac{\bar{c}\,(1-\bar{c})}{\sqrt{\Gamma_0}} A_n \tag{5}$$

where $\bar{c}$ is the average composition of the solution. To test our model, we performed calculations with different noise levels. For each fixed noise we started from a homogeneous solution, the mean square fluctuation of composition $\sqrt{\langle(\delta c)^2\rangle}$ started to grow with time from zero and eventually reached asymptotic value. We plotted these asymptotic values of $\sqrt{\langle(\delta c)^2\rangle}$ vs. A_n. As can be seen in Fig. 1, the results fulfilled perfectly the interrelation (5). Note that this calculation was repeated for different $\bar{c}$ values and computation cell sizes.

Table 1
Analysis of the KMC results. At the end of each KMC run, a value of 1, 0 or 0.5 was assigned to the lattice sites, depending on if the site is occupied by an *A*, *B* atom or a vacancy, respectively. The bottom line shows the average value of each site and dispersion of the averages.

	Site 1	Site 2	Site 3	…	Site 500	
MC run 1	0	1	1	…	1	
MC run 2	1	1	0	…	1	
MC run 3	1	1	1	…	0	
⋮				…		
MC run *N*	0	0	1	…	0	
Average	0.5132	0.5113	0.5049	…	0.4992	$\sigma_{KMC} = 4.961 \times 10^{-3}$

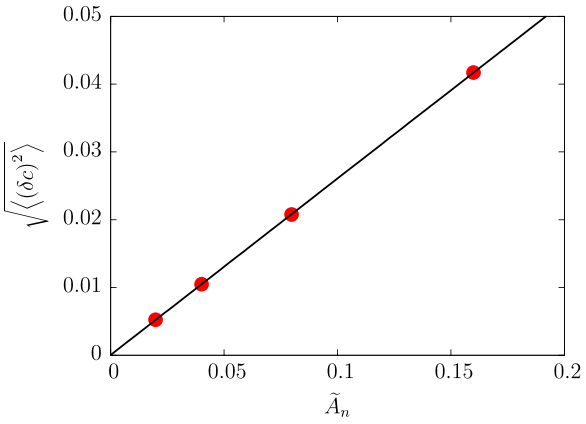

Fig. 1. Steady-state deviation of the composition as a function of noise amplitude: $\sqrt{\langle(\delta c)^2\rangle}$ vs. $\tilde{A}_n$ with $\bar{c} = 0.5$ and $\tilde{\Gamma} = 1$. The computational cell was a cube containing $60 * 60 * 60/2$ atoms in FCC structure; periodic boundary condition was applied. The data points fit to a straight line with a slope of 0.25. (see Eq. (5)).

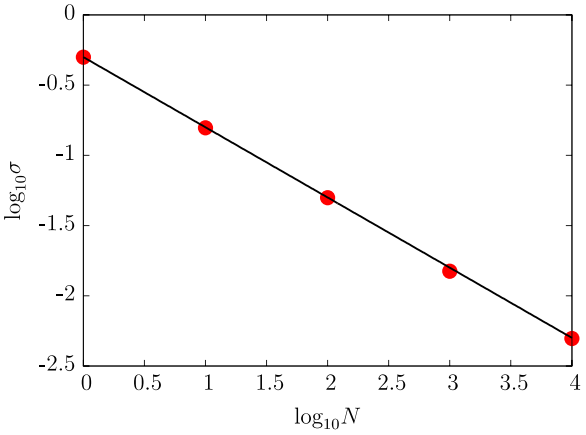

Fig. 2. Dispersion of the composition from the average of *N* KMC runs as a function of *N* on the $\log_{10}$–$\log_{10}$ scale. The slope of the fitted straight line is −0.5 and the *y*-intercept is −0.3.

We also performed these calculations by using a one-vacancy KMC [13] in the equiatomic alloy. There were 500 atoms in the computation cell. The lattice was FCC and periodic boundary condition was applied. We repeated the simulation 10^4 times always starting from the same random configuration. Each simulation consisted of 80 Monte Carlo steps. At the end of each KMC run, we assigned a number to the sites: 1 if the site was occupied by *A*, 0 if by *B* and 0.5 if by the vacancy. We averaged the value of each corresponding site for *N* runs resulting 500 values scattering around 0.5 (see Table 1) – the higher the *N*, the closer to 0.5. Then we calculated the dispersion (σ_{KMC}) of these 500 values. We performed this for *N* equal to 1, 10, 100, 1000 and 10000. Fig. 2 shows the σ_{KMC} as a function of *N*.

As can be seen, the data points fit perfectly to a straight line on the $\log_{10}$–$\log_{10}$ scale of which slope is equal to −0.5. The *y*-intercept is equal to −0.3 ($\log_{10} 0.5$), which is obvious as for $N = 1$, $\sigma_{KMC} = 0.5$ (dispersion of the same number of 1s and 0s). Therefore,

$$\sigma_{KMC} = \frac{1}{2\sqrt{N}}. \tag{6}$$

As shown in Appendix B, this formula can also be easily derived analytically. In case of arbitrary composition $\bar{c}$, instead of Eq. (6) one has

$$\sigma_{KMC} = \sqrt{\bar{c}\,(1-\bar{c})}\,\frac{1}{\sqrt{N}}. \tag{6'}$$

As can be seen for $N \to \infty$, $\sigma_{KMC} \to 0$. This means that after averaging an infinite number of KMC runs the dispersion of the site averages is equal to zero; which is just the result of an SKMF with $A_n = 0$ (i.e. a KMF). This means that it is reasonable to try to find some relation between *N* and A_n. This can be done by comparing Eqs. (5) and (6′) ($\sqrt{\langle(\delta c)^2\rangle} = \sigma_{KMC}$):

$$N = \frac{\Gamma_0}{\bar{c}\,(1-\bar{c})\,A_n^2}. \tag{7}$$

This formula (as already mentioned, its analytical derivation is given in Appendix B) gives, therefore, how many times a KMC calculation should be run and averaged to get the same result as an SKMF run gives with a given A_n; or inversely, an SKMF run with a given A_n equal to the average of how many KMC runs. This clearly shows the high efficiency of SKMF. If we also consider that usually one SKMF run is much faster than one KMC run, the gain is invaluable.

Expression (7) also shows that by varying the value of A_n, an SKMF calculation can be literally tuned between KMC and KMF limits, as desired.

To check and illustrate the effectiveness of SKMF, we applied it to the following examples: (I) nucleation and decomposition in the metastable solid solution; (II) influence of noise on the spinodal decomposition in quasi-1D structure (nanowire).

(I) As mentioned in the introduction, noise is especially important for first-order phase transitions which require overcoming of nucleation barriers. Therefore we started checking SKMF by modeling of decomposition of a solid solution at a given temperature and composition corresponding to a metastable state (between the spinodal and the solubility curves-Fig. 3a–b). Of course, without noise (i.e. within KMF model) the initially homogeneous alloy will remain unchanged forever.

We introduced the Langevin noise of various amplitudes. As expected, this provided the nucleation (homogeneous one) and growth after some waiting (incubation) time. Characteristic videos demonstrating nucleation and growth are provided in Supplementary materials [14] (Movie 1, Appendix C). Although, strictly speaking, the exact moment of nucleation is ambiguous,

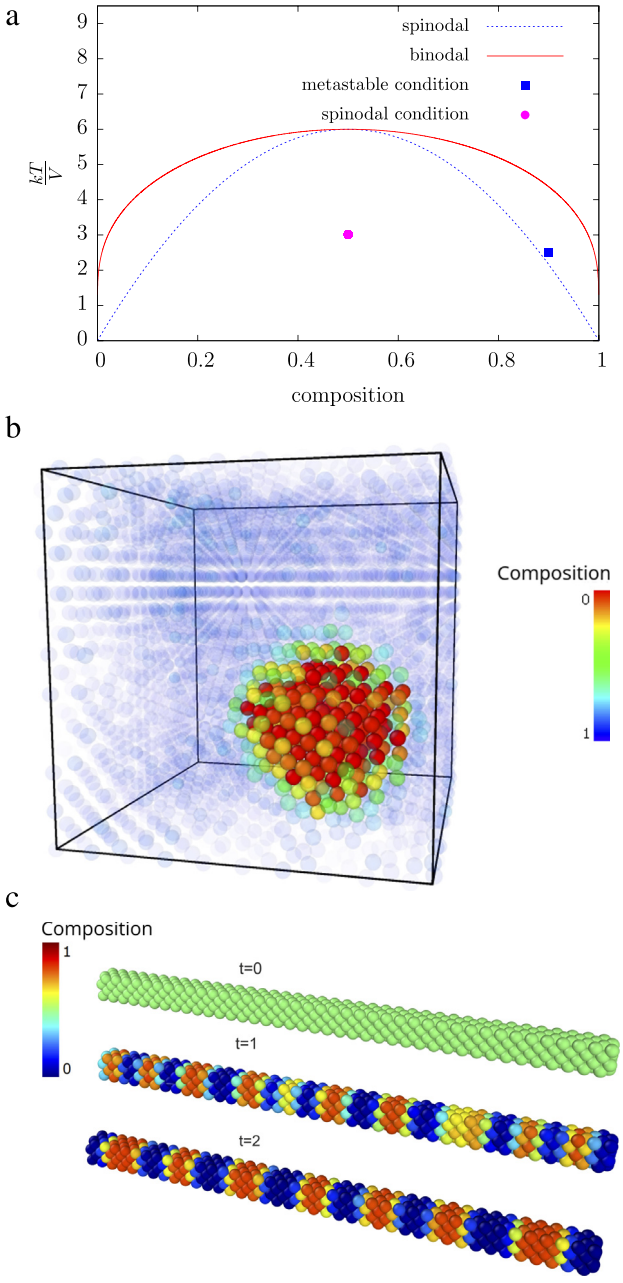

Fig. 3. (a) Phase diagram of the modeled binary solid solution system (dimensionless temperature on the vertical axes). Dashed blue and continuous red lines correspond to the spinodal and miscibility curves respectively. The blue square ($\bar{c} = 0.9$; $V/kT = 0.4$) indicates the initial state of the system in the metastable region for single nucleation process. The magenta filled circle ($\bar{c} = 0.5$; $V/kT = 0.3316$) indicates the initial state of the system for the spinodal decomposition process of nanowire. (b) Nucleation during decomposition in metastable binary solid solution. Calculation conditions: mean composition $\bar{c} = 0.9$; mixing energy $V/kT = 0.4$; noise amplitude $\tilde{A}_n = 0.5$; sample size $20\times20\times20$. (c) Spinodal decomposition in quasi-1D structure (nanowire). Initial conditions: mean composition $\bar{c} = 0.5$; mixing energy $V/kT = 0.3316$; sample size $80\times4\times4$; dynamic noise with amplitudes $\tilde{A}_n = 0.1$ was used. (For interpretation of the references to color in this figure legend, the reader is referred to the web version of this article.)

the time of rapid cluster growth after overcoming the nucleation barrier is much shorter than the waiting time before overcoming. Therefore the criterion of nucleation may be varied. A careful analysis of incubation time versus noise amplitude will be discussed elsewhere.

(II) To start the spinodal decomposition, even the smallest deviation of composition from homogeneous value is sufficient.

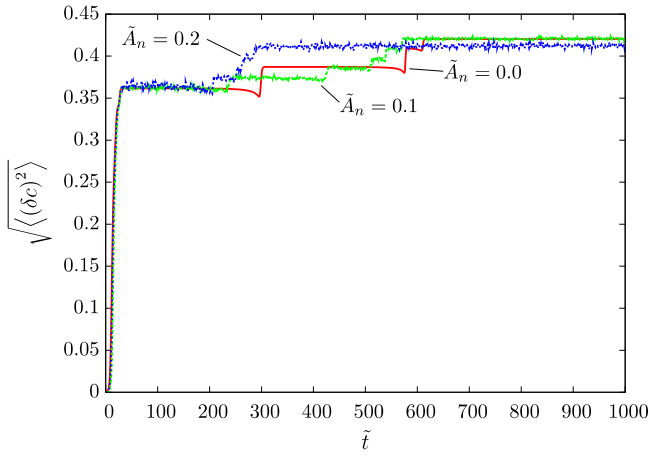

Fig. 4. Time dependence of composition deviation for different dynamic noise amplitudes. All coagulation events correspond to the steps on the time dependences of composition deviation (see also the corresponding Movies in Supplementary material [14]).

Accordingly, at the initial stage the noise is not that important. Yet, the late stages become much more interesting, especially in 1D. It can be predicted that in thin long nanowires with radius less than Cahn's characteristic length of spinodal decomposition the lamellar structure formation is possible only along the axis of the nanowires. Roughening of this structure cannot proceed by ordinary Ostwald ripening, because all interfaces are practically planar, so that Gibbs-Thomson effect cannot play any role. Nevertheless, one can observe "stochastic-like" roughening consisting of "coagulation events" happening from time to time between the nearest particles along the axis (see Fig. 4 and Movie 2 in Supplementary material [14]). This process depends on the noise level: the higher the noise amplitude, the faster the sequence of coagulation events.

5. Conclusions and summary

In this work, we presented a new method, called Stochastic Kinetic Mean Field (SKMF), for atomistic modeling of diffusion-controlled processes. We demonstrated how efficient SKMF is. The code using the direct atomic exchange mechanism of diffusion is available at the http://skmf.eu [13] website.

We also demonstrated that the model could be generalized to the vacancy mechanism. We proposed a workaround for the problem that, usually, simulation time with the vacancy mechanism – instead of the direct atomic exchange – increases significantly. We are working on the implementation and testing of the code and will publish it as well as make it available on the http://skmf.eu website.

Besides the vacancy mechanism, SKMF could also be generalized for ternary (etc.) systems. Note that for these generalized cases SKMF will be even more efficient compared to KMC.

We intend to keep developing the model and then publish the codes of the new algorithms as open source. [13] In particular, the dependence of nucleation rate in metastable solid solution on noise amplitude, as well as on supersaturation will be discussed elsewhere. The nucleation of intermediate phases will be studied by SKMF in bulk samples, in nanofilms and nanoclusters, as well as at interfaces and in nanosized contact zones with sharp concentration gradients. Also, competitive ordering on FCC lattice in bulk samples, diffusion couples, nanofilms and nanoclusters will be studied in detail, with account of segregation at interfaces due to diffusion asymmetry ($M \neq 0$).

Acknowledgments

This work was supported in part by the OTKA Board of Hungary (No. NF101329), by Ministry of Education and Science of Ukraine (project 0115 U 000638), by EXMONAN EU FP7 project (Ref. 612552) and by TAMOP 4.2.2.A-11/1/KONV- 2012-0036 project entered through the New Hungary Development Plan co-financed by the European Social Fund, and the European Regional Development Fund. For 3D visualization we used OVITO [11].

Author contributions statement: A.M.G. and Z.E. conceived the project; A.M.G., M.P. and Z.E. provided the theoretical considerations; J.J.T., M.P., V.B., B.G. and Z.E. wrote and tested the program codes, analyzed and plotted the simulation results; A.M.G., J.J.T. and Z.E. wrote and formatted the manuscript. The authors would like to thank Louis J. Mattia for proofreading of the article.

Appendix A. Derivation of interrelation between noise amplitude and composition fluctuations for the simplest case of ideal symmetric solution ($V = 0$, $M = 0$).

$$\begin{aligned}\frac{dc_i}{dt} &= -\sum_{j=1}^{Z}\Big[c_i\left(1-c_j\right)\left(\Gamma_{i,j}^{mean\text{-}field}+\delta\Gamma_{i,j}^{Lang}\right)\\ &\quad-\left(1-c_i\right)c_j\left(\Gamma_{j,i}^{mean\text{-}field}+\delta\Gamma_{j,i}^{Lang}\right)\Big] \qquad (A.1)\\ \frac{d\bar{c}}{dt} &= 0.\end{aligned}$$

Let us trace the evolution of fluctuation.

$$\begin{aligned}\frac{d\delta c_i}{dt} &= \frac{dc_i}{dt}-\frac{d\bar{c}}{dt} = -\sum_{j=1}^{Z}\left(\bar{c}+\delta c_i\right)\left(1-\bar{c}-\delta c_j\right)\left(\Gamma_0+\delta\Gamma_{i,j}^{Lang}\right)\\ &\quad+\sum_{j=1}^{Z}\left(\bar{c}+\delta c_j\right)\left(1-\bar{c}-\delta c_i\right)\left(\Gamma_0+\delta\Gamma_{j,i}^{Lang}\right)\\ &= -Z\Gamma_0\delta c_i+\Gamma_0\sum_{j=1}^{Z}\delta c_j+\bar{c}\left(1-\bar{c}\right)\sum_{j=1}^{Z}\left(\delta\Gamma_{j,i}^{Lang}-\delta\Gamma_{i,j}^{Lang}\right)\\ &\quad+O\left(\delta^2\right).\end{aligned}$$

Thus, linearized kinetic equations for the fluctuations of composition will have the following form:

$$\begin{aligned}\frac{d\delta c_i}{dt} &\approx -Z\Gamma_0\delta c_i+\Gamma_0\sum_{j=1}^{Z}\delta c_j\\ &\quad+\bar{c}\left(1-\bar{c}\right)\sum_{j=1}^{Z}\left(\delta\Gamma_{j,i}^{Lang}-\delta\Gamma_{i,j}^{Lang}\right). \qquad (A.2)\end{aligned}$$

Multiply both sides of Eq. (A.2) on the δc_i and make averaging over ensemble, using relations

$$\langle\delta c_i\rangle = 0, \qquad \langle\delta c_j\rangle = 0, \qquad \langle\delta c_i\delta c_j\rangle = 0 \qquad (A.3)$$

(for ideal solution there is no correlation between different sites)

$$\begin{aligned}\left\langle\delta c_i\frac{d\delta c_i}{dt}\right\rangle &= -Z\Gamma_0\langle(\delta c_i)^2\rangle+\Gamma_0\sum_{j=1}^{Z}\langle\delta c_i\delta c_j\rangle\\ &\quad+\bar{c}\left(1-\bar{c}\right)\sum_{j=1}^{Z}\left\langle\delta c_i\left(\delta\Gamma_{j,i}^{Lang}-\delta\Gamma_{i,j}^{Lang}\right)\right\rangle\\ \frac{d\langle\delta c_i^2\rangle}{dt} &= 0 = -Z\Gamma_0\langle(\delta c)^2\rangle\\ &\quad+\bar{c}\left(1-\bar{c}\right)\sum_{j=1}^{Z}\left\langle\delta c_i\left(\delta\Gamma_{j,i}^{Lang}-\delta\Gamma_{i,j}^{Lang}\right)\right\rangle.\end{aligned}$$

Thus,

$$\sum_{j=1}^{Z}\left\langle\delta c_i\left(\delta\Gamma_{j,i}^{Lang}-\delta\Gamma_{i,j}^{Lang}\right)\right\rangle = \frac{Z\Gamma_0}{\bar{c}\left(1-\bar{c}\right)}\langle(\delta c)^2\rangle. \qquad (A.4)$$

Langevin noise of exchange rates means:

$$\begin{aligned}\langle\delta\Gamma_{j,i}^{Lang}(t)\,\delta\Gamma_{m,i}^{Lang}\left(t'\right)\rangle &= A_n^2\delta_{jm}\delta\left(t-t'\right),\\ \langle\delta\Gamma_{i,k}^{Lang}(t)\,\delta\Gamma_{i,m}^{Lang}\left(t'\right)\rangle &= A_n^2\delta_{km}\delta\left(t-t'\right).\end{aligned} \qquad (A.5)$$

Set of Eq. (A.2) for the composition fluctuations in all sites can be rewritten in the following form:

$$\frac{d\delta c_i}{dt} \approx -\sum_k M_{ik}\delta c_k+f_i(t). \qquad (A.6)$$

Or, in column-matrix notations,

$$\frac{d\delta\hat{c}}{dt} \approx -\hat{M}\delta\hat{c}+\hat{f}(t). \qquad (A.7)$$

Now consider δc_i as a formal solution of Eq. (A.7) with zero initial condition (which will be relaxed to zero anyway),

$$\delta\hat{c}(t) = \int_0^t\exp\left(-\left(t-t'\right)\hat{M}\right)\hat{f}\left(t'\right)dt', \qquad (A.8)$$

where

$$f_i(t) = \bar{c}\left(1-\bar{c}\right)\sum_{k=1}^{Z}\left(\delta\Gamma_{k,i}^{Lang}-\delta\Gamma_{i,k}^{Lang}\right). \qquad (A.9)$$

Here exponent of the matrix means the Taylor series expansion:

$$\exp\left(-\left(t-t'\right)\hat{M}\right) = 1+\sum_{n=1}^{\infty}(-1)^n\frac{\left(t-t'\right)^n}{n!}\hat{M}^n,$$

and product of matrices and column is a matrix product.

Most important for us is that the matrix function $\exp(-(t-t')\hat{M})$ tends to unit operator (just number 1) when t' tends to t this is important due to absence of memory in Langevin noise.

Now substitute Eqs. (A.8), (A.9) into Eq. (A.4) with account of Langevin conditions (A.5):

$$\begin{aligned}\frac{Z\Gamma_0}{\bar{c}\left(1-\bar{c}\right)}\langle(\delta c)^2\rangle &= \sum_{j=1}^{Z}\left\langle\delta c_i\left(\delta\Gamma_{j,i}^{Lang}-\delta\Gamma_{i,j}^{Lang}\right)\right\rangle\\ &= \sum_{j=1}^{Z}\left\langle\int_0^t\exp\left(-\left(t-t'\right)\hat{M}\right)\hat{f}\left(t'\right)dt'\right.\\ &\quad\left.\times\left(\delta\Gamma_{j,i}^{Lang}(t)-\delta\Gamma_{i,j}^{Lang}(t)\right)\right\rangle\\ &= \bar{c}\left(1-\bar{c}\right)\sum_{j=1}^{Z}\left\langle\int_0^t dt'\exp\left(-\left(t-t'\right)\hat{M}\right)\right.\\ &\quad\times\sum_{m=1}^{Z}\left(\delta\Gamma_{m,i}^{Lang}\left(t'\right)-\delta\Gamma_{i,m}^{Lang}\left(t'\right)\right)\\ &\quad\left.\times\left(\delta\Gamma_{j,i}^{Lang}(t)-\delta\Gamma_{i,j}^{Lang}(t)\right)\right\rangle\\ &= \bar{c}\left(1-\bar{c}\right)\sum_{j=1}^{Z}\sum_{m=1}^{Z}\int_0^t dt'\exp\left(-\left(t-t'\right)\hat{M}\right)\\ &\quad\times\left\langle\left(\delta\Gamma_{m,i}^{Lang}\left(t'\right)-\delta\Gamma_{i,m}^{Lang}\left(t'\right)\right)\left(\delta\Gamma_{j,i}^{Lang}(t)-\delta\Gamma_{i,j}^{Lang}(t)\right)\right\rangle\\ &= \left(1-\bar{c}\right)\sum_{j=1}^{Z}\sum_{m=1}^{Z}\int_0^t dt'\exp\left(-\left(t-t'\right)\hat{M}\right)\\ &\quad\times\left(A_n^2\delta_{jm}\delta\left(t-t'\right)-0-0+A_n^2\delta_{jm}\delta\left(t-t'\right)\right). \qquad (A.10)\end{aligned}$$

Now take into account that

$$\int_0^t g\left(t-t'\right)\delta\left(t-t'\right)dt' = \frac{1}{2}g\left(0\right). \tag{A.11}$$

Thus

$$\begin{aligned}\frac{Z\Gamma_0}{\bar{c}\left(1-\bar{c}\right)}\langle(\delta c)^2\rangle &= \bar{c}\left(1-\bar{c}\right)\\ &\times\sum_{j=1}^{Z}\sum_{m=1}^{Z}\left(\frac{1}{2}A_n^2\delta_{jm}-0-0+\frac{1}{2}A_n^2\delta_{jm}\right)\\ &= \bar{c}\left(1-\bar{c}\right)ZA_n^2.\end{aligned}$$

Then

$$\langle(\delta c)^2\rangle = \left(\bar{c}\left(1-\bar{c}\right)\right)^2\frac{1}{\Gamma_0}A_n^2. \tag{A.12}$$

Note once more that A_n in Eq. (A.12) is amplitude, which in discrete scheme is a coefficient in Eq. (4) in the main text:

$$\delta\Gamma_{i,j}^{Lang} = \frac{A_n}{\sqrt{dt}}\sqrt{3}\left(2\cdot random-1\right). \tag{A.13}$$

Appendix B. Interrelation between KMC and SKMF

Let X_n be equal to 1 if after nth Monte Carlo run a given site will contain atom A and be equal to 0 if it contains atom B (we will neglect here the probability of vacancy). Evidently, the probability of first event is just composition $\bar{c}$, probability of alternative event is $1-\bar{c}$. Then the mean values of the random entities X_n and X_n^2 are following:

$$\begin{aligned}\langle X_n\rangle &= 1\cdot\bar{c}+0\cdot\left(1-\bar{c}\right)=\bar{c},\\ \langle X_n^2\rangle &= 1^2\cdot\bar{c}+0^2\cdot\left(1-\bar{c}\right)=\bar{c}.\end{aligned} \tag{B.1}$$

Since the different Monte Carlo runs are fully uncorrelated, one can expect that

$$\langle X_nX_k\rangle|_{n\neq k} = \langle X_n\rangle\langle X_k\rangle = \bar{c}\cdot\bar{c} = \bar{c}^2. \tag{B.2}$$

Then the variance (square of deviation)

$$\begin{aligned}\sigma_{KMC}^2 &= \langle(c-\bar{c})^2\rangle = \langle(c)^2-2\langle c\rangle\bar{c}+\bar{c}^2\rangle = \langle(c)^2\rangle-\bar{c}^2\\ &= \left\langle\left(\frac{\sum_{n=1}^{N}X_n}{N}\right)^2\right\rangle-\bar{c}^2 = \left(\frac{\sum_{n=1}^{N}\langle(X_n)^2\rangle}{N^2}+\frac{\sum_{n\neq k}\sum\langle X_nX_k\rangle}{N^2}\right)-\bar{c}^2\\ &= \left(\frac{N\bar{c}}{N^2}+\frac{\left(N^2-N\right)\bar{c}^2}{N^2}\right)-\bar{c}^2 = \frac{\bar{c}\left(1-\bar{c}\right)}{N}.\end{aligned} \tag{B.3}$$

This gives us Eq. (6′) of the main text. We remind here that N is a number of runs of KMC.

On the other hand, as shown in Discussion 1 (see Eq. (A.12)), the variance in SKMF method for the ideal solution is

$$\langle(\delta c)^2\rangle \equiv \sigma_{SKMF}^2 = \frac{\left(\bar{c}\left(1-\bar{c}\right)\right)^2}{\Gamma_0}A_n^2. \tag{B.4}$$

Equalizing $\sigma_{SKMF}^2=\sigma_{KMC}^2$, one gets:

$$N = \frac{\Gamma_0}{\bar{c}\left(1-\bar{c}\right)A_n^2} \tag{B.5}$$

which is Eq. (7) in the main text.

Appendix C. Supplementary material

Supplementary material related to this article can be found online at http://dx.doi.org/10.1016/j.cpc.2016.03.003.

References

[1] A. Khachaturyan, Theory of Structural Transformations in Solids, Dover Publications, 2013.
[2] Y. Wang, L. Chen, A. Khachaturyan, Computer simulation of microstructure evolution in coherent solids, in: Solid-to-Solid Phase Transformations, PTM'94, 1994, pp. 245–265;
Y. Wang, D. Banerjee, C.C. Su, A.G. Khachaturyan, Field kinetic model and computer simulation of precipitation 2 ordered intermetallics from fcc solid solution, Acta Mater. 46 (9) (1998) 2983–3001.
[3] L. Chen, J. Simmons, Microscopic master equation approach to diffusional transformations in inhomogeneous systems – single-site approximation and direct exchange mechanism, Acta Metall. Mater. 3 (1994) 2943–2954.
[4] G. Martin, Atomic mobility in Cahn's diffusion model, Phys. Rev. B 4 (1990) 2279–2283.
[5] Z. Erdélyi, et al., Transient interface sharpening in miscible alloys, Science 5 (2004) 1913–1915.
[6] Z. Erdélyi, I. Szabó, D. Beke, Interface sharpening instead of broadening by diffusion in ideal binary alloys, Phys. Rev. Lett. 89 (2002).
[7] Z. Erdélyi, D. Beke, A. Taranovskyy, Dissolution and off-stoichiometric formation of compound layers in solid state reactions, Appl. Phys. Lett. 92 (2008) 133110.
[8] N. Storozhuk, K. Sopiga, A. Gusak, Mean-field and quasi-phase-field models of nucleation and phase competition in reactive diffusion, Phil. Mag. 93 (2013) 1999–2012.
[9] F. Soisson, G. Martin, Monte Carlo simulations of the decomposition of metastable solid solutions: Transient and steady-state nucleation kinetics, Phys. Rev. B 62 (2000) 203–214.
[10] I. Vernyhora, D. Ledue, R. Patte, H. Zapolsky, Monte Carlo investigation of the correlation between magnetic and chemical ordering in NiFe alloys, J. Magn. Magn. Mater. 322 (2010) 2465–2470.
[11] A. Stukowski, Visualization and analysis of atomistic simulation data with OVITO – the open visualization tool, Modelling Simulation Mater. Sci. Eng. 18 (2009) 015012.
[12] Z. Erdélyi, Z. Balogh, D. Beke, Kinetic critical radius in nucleation and growth processes – Trapping effect, Acta Mater. 12 (2010) 5639–5645.
[13] SKMF website: http://skmf.eu.
[14] See Supplementary material at http://dx.doi.org/10.1016/j.cpc.2016.03.003 for additional example videos and textual discussions.